

Simulation of Heat Transport Across Magnetic Islands in TEXTOR

M. Hölzl¹, S. Günter¹, I. G. J. Classen^{1,2}, Q. Yu¹, TEXTOR Team³, E. Delabie²

¹ Max-Planck-Institut für Plasmaphysik, EURATOM Association, 85748 Garching, Germany

² FOM-Institute for Plasma Physics Rijnhuizen, Association EURATOM-FOM, Trilateral Euregio Cluster, PO Box 1207, 3430 BE Nieuwegein, The Netherlands, www.rijnhuizen.nl

³ Institut für Energieforschung-Plasmaphysik, Forschungszentrum Jülich GmbH, EURATOM Association, Trilateral Euregio Cluster, 52425 Jülich, Germany

Introduction

Heat transport in magnetised plasmas is faster along magnetic field lines than perpendicular to them by many orders of magnitude [1], which brings about a flattening of the temperature profile inside magnetic islands [2]. The ratio between the parallel and perpendicular heat diffusivities, $\chi_{\parallel}/\chi_{\perp}$, is not easily accessible in experiments despite its important role for the dynamics of neoclassical tearing modes. In this article, we systematically compare measurements of the temperature distribution around a magnetic island to numerical simulations that are performed with the methods developed in Ref. [3] and are capable of treating realistic values of the heat diffusion anisotropy in toroidal geometries [4]. We present a method to determine the experimental heat diffusion anisotropy and the magnetic island size from this comparison. The investigations are described in more detail in Ref. [5].

The method is applied to a 2/1 magnetic island triggered by the dynamic ergodic divertor (DED) coil set [6] in TEXTOR. The electron temperature around the island, measured by electron cyclotron emission imaging (ECE-Imaging) [7], is compared to the numerical simulation results.

Experiment

TEXTOR discharge #99175, which is characterised by a magnetic field strength of 2.25T and a plasma current of about 300kA, is studied. At $t = 1.6$ s, the plasma is heated by roughly 250kW of Ohmic heating and about 300kW of neutral beam injection heating. Perturbation fields can in TEXTOR be produced by the 16 helical DED coils. The principal component is selected to be the 3/1 mode in our case which has a strong 2/1 sideband. The perturbation rotates around the torus as the coils are fed with a 1kHz AC current and gives rise to a 2/1 magnetic island as the coil currents are ramped up. This island will be used for our comparison during its growth phase after the mode has locked. Radial profiles of the 2/1 magnetic perturbation are derived from nonlinear cylindrical two-fluid MHD

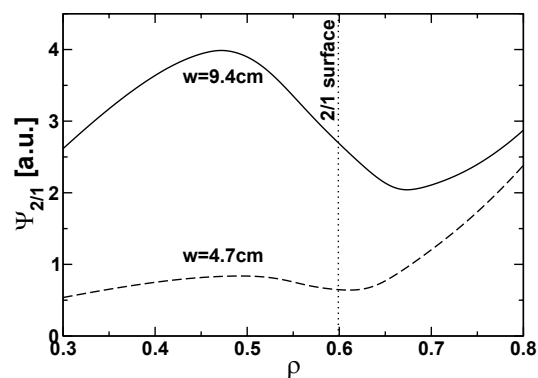


Figure 1: Radial profiles of the 2/1 magnetic perturbation for two different perturbation amplitudes are shown.

simulations that are performed for typical TEXTOR parameters analogous to Ref. [8] and do not rely on the so-called vacuum assumption but include the full plasma interaction with the external magnetic perturbation. Profiles for two different island sizes are depicted in Fig. 1.

The electron temperature around the island is measured by TEXTOR's ECE-Imaging diagnostic [7] which consists of an array of 8 radial times 16 vertical channels, which are located around the outer mid-plane for this shot. Thermal noise is suppressed by singular value decomposition. Assuming rigid body rotation, each channel provides data corresponding to a toroidal resp. poloidal temperature profile at a different radial position. About 100 data points are available per mode transit around the torus. Six channels located at $Z = 0$ close to the 2/1 resonant surface are selected. The ECEI signals are first cross-calibrated against the 1D ECE diagnostic and then calibrated relatively. This calibration is kept fixed for all cases considered.

Physics Model

As the island evolution is slow enough such that the temperature distribution can be assumed to follow changes of the magnetic topology instantaneously, we model the electron heat transport by the steady-state anisotropic heat diffusion equation, $\nabla \cdot \mathbf{q}_e = P_e$, where $\mathbf{q}_e = -n_e [\chi_{\parallel,e} \nabla_{\parallel} T_e + \chi_{\perp,e} \nabla_{\perp} T_e]$ is the heat flux density, n_e denotes the electron particle density, P_e the energy source term, $\nabla_{\parallel} T_e$ the temperature gradient parallel to the magnetic field lines, and $\nabla_{\perp} T_e$ the cross-field temperature gradient. The energy source term, P_e , is set to half of the sum of Ohmic and NBI heating powers.

Our computations are performed with the finite difference scheme developed in Ref. [3] that can treat realistic heat diffusion anisotropies without full alignment of the coordinates to the magnetic field lines in toroidal geometries [4]. An unshered helical coordinate system aligned to the 2/1 island is used to reduce the necessary toroidal resolution. For details on the tensorial form of the heat diffusion equation and the helical coordinate system, refer to Ref. [4]. The profile of the unperturbed cross-field heat diffusion coefficient, $\chi_{\perp,e}$, can be determined from the heating power deposition profile and the temperature profile measured prior to the onset of the magnetic island. At the 2/1 resonant surface, $\chi_{\perp,e}$ takes a value of about $0.9 \text{ m}^2/\text{s}$. We assume that the island does not alter the profile significantly. Inside magnetic islands, the perpendicular heat diffusion coefficient may, however, differ from outside the island. Examinations with local heating into the island are planned to be considered for studying this.

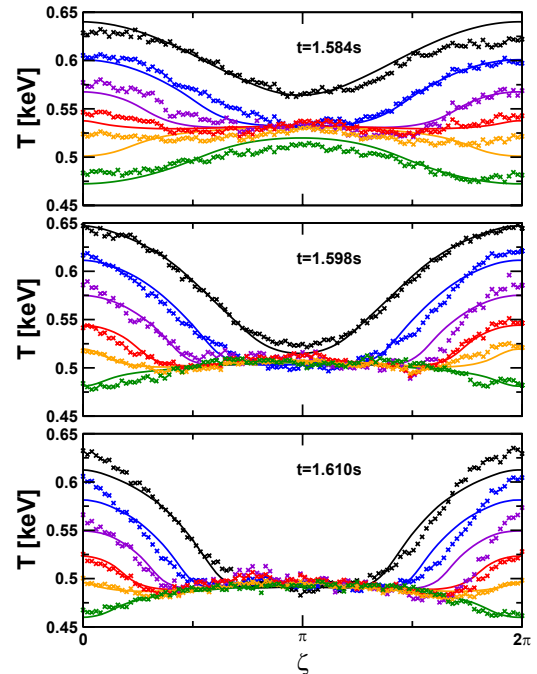


Figure 2: Comparisons of experimental (“x”) and numerical (solid lines) temperature profiles. The island O-point is located at $\zeta = \pi$.

Comparison between simulations and measurements

Our method is now applied to TEXTOR discharge #99175. Calculations are performed for various values of island width and heat diffusion anisotropy. For each mode-transit around the torus, the simulation is selected that reproduces the measured temperature profiles best as indicated by the smallest quadratic deviations. The matching algorithm is described in detail in Ref. [5]. The “numerical temperature signals” that are compared to the experiment are toroidal profiles determined at the outer mid-plane.

Very good agreement between numerical and experimental data is obtained in the time-interval $t = 1.584\text{s} \dots 1.610\text{s}$ which will be used for the determination of $\chi_{\parallel}/\chi_{\perp}$. For three representative time-points, the experimental and numerical data sets are compared in Fig. 2. The quadratic difference, Q , between the measured and calculated temperature profiles is plotted in Figure 3. The strongly increased error prior to the considered time-interval are caused by irregularities in the ECEI signals. After $t = 1.61\text{s}$, the island has become larger than 20 percent of the minor radius which cannot be simulated reasonably with the magnetic perturbation model used as stochasticity arises that is absent in the experiment due to shielding currents.

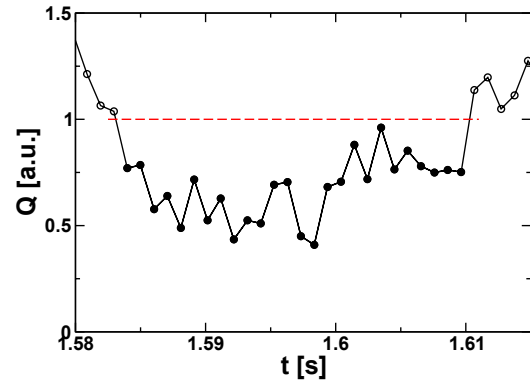


Figure 3: Discrepancy between numerical and experimental temperature profiles.

The sensitivity of the simulated temperature signals on variations of the island width and the heat diffusion anisotropy were studied showing that the detected values of the island width for every single mode-transit around the torus are reliable to $\pm 0.5\text{cm}$ and these of the heat diffusion anisotropy to a factor smaller than 5.

The matching procedure is now applied to the temperature measurements of many mode transits around the torus. Thus, time-traces of the island width and the heat diffusion anisotropy are obtained. From Figure 4, the magnetic island width can be seen to increase from about 5.5cm to 9.5cm. The heat diffusion anisotropy fluctuates around 10^8 which corresponds to a value of w/w_c that increases from 3 to 5.

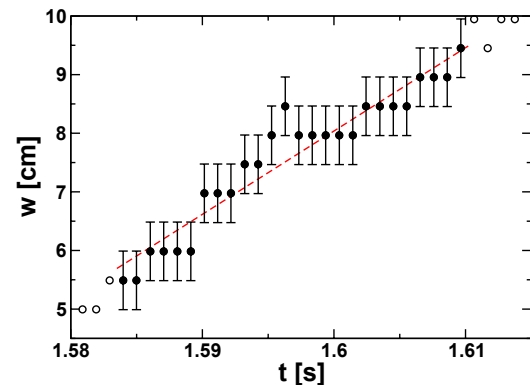


Figure 4: In the considered time-interval, the island grows from about 5.5 to 9.5cm.

The distribution of the values obtained for the heat diffusion anisotropy is analysed in Figure 5. We get the value $\chi_{\parallel}/\chi_{\perp} = 10^8$ with an uncertainty factor of about 3. Due to the large number of “measurements” of the heat diffusion anisotropy, the uncertainty is somewhat smaller than that estimated for the single mode-transits above.

Discussion

Outside the island heat conduction layer, the temperature is constant within each flux surface irrespective of the exact value of the heat diffusion anisotropy. We have consequently determined an effective heat diffusion anisotropy of the heat conduction layer. According to Spitzer and Härm [1], an anisotropy around $4 \cdot 10^9$ would be expected, which is by a factor of 40 larger than what we observe. This is an indication for the heat flux limit that was first derived by Malone, McCrory and Morse [9]. It predicts the same heat diffusion anisotropy as Spitzer-Härm in a thin layer ($\lesssim 1\text{mm}$)

around resonant surfaces and island separatrices, but values reduced by 1 or 2 orders of magnitude apart from these. In the considered discharge, the width of the heat conduction layer is roughly between 0.5cm and 2cm according to Ref. [2]. Thus, the anisotropy is predicted to be much lower than the Spitzer-Härm level over most of the heat conduction layer according to heat flux limit theory. Qualitatively, this agrees very well with our observation that the effective heat diffusion anisotropy in the heat conduction layer is much lower than the Spitzer-Härm level. An indication for the heat flux limit has previously also been found in Ref. [10].

Summary

A method for the determination of the magnetic island size and the heat conduction anisotropy by comparing results of heat diffusion simulations to temperature measurements has been developed. An algorithm automatically detects the numerical temperature profiles that reproduce the measurements best. For the 2/1 island in TEXTOR considered, the island width increases from $w = 5.5\text{cm}$ to 9.5cm at a growth rate of 1.5m/s while the ratio w/w_c increases from 3 to 5. A heat diffusion anisotropy of 10^8 is observed with an uncertainty factor of 3. This is lower than the Spitzer-Härm prediction by a factor of 40 and supports heat flux limit theories.

References

- [1] L. Spitzer and R. Härm. *Phys. Rev.*, **89** (1953), 997.
- [2] R. Fitzpatrick. *Phys. Plasmas*, **2** (1995), 825.
- [3] S. Günter, Q. Yu, et al. *J. Comput. Phys.*, **209** (2005), 354.
- [4] M. Hölzl, S. Günter, and ASDEX Upgrade Team. *Phys. Plasmas*, **15** (2008), 072514.
- [5] M. Hölzl, S. Günter, et al. *Nucl. Fusion*, **to be published** (2009).
- [6] *Special Issue, Fusion Eng. Design*, **37** (1997), 335. Edited by K. H. Finken.
- [7] H. Park, C. C. Chang, et al. *Rev. Sci. Instrum.*, **74** (2003), 4239.
- [8] Q. Yu, S. Günter, and K. H. Finken. *Phys. Plasmas*, **16** (2009), 042301.
- [9] R. C. Malone, R. L. McCrory, and R. L. Morse. *Phys. Rev. Lett.*, **34** (1975), 721.
- [10] M. Z. Tokar and A. Gupta. *Phys. Rev. Lett.*, **99** (2007), 225001.

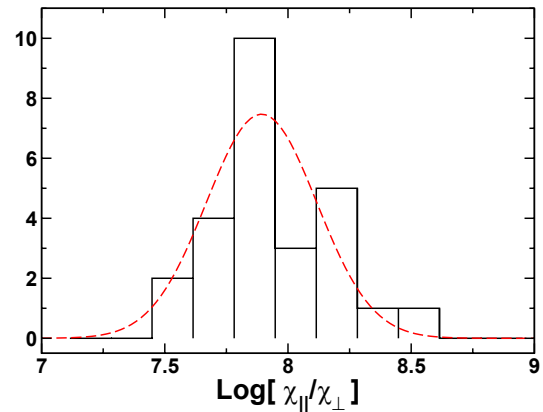


Figure 5: Distribution of the obtained values for the heat diffusion anisotropy.